



EPTT-2020-0121

A STUDY ON THREE-DIMENSIONAL AND ISOLATED ROUGHNESS INDUCED TRANSITION

Ana Elisa Basilio de Carvalho¹

Fernando H T Himeno²

Marlon Sproesser Mathias³

Marcello Augusto Faraco de Medeiros⁴

^{1 2 3 4} São Carlos School of Engineering, University of São Paulo, EESC-USP.

¹ anaelisabasilio@usp.br, ⁴ marcello@sc.usp.br

Abstract. *The nonlinear instability and transition to turbulent flow are investigated through a Direct Numerical Simulation of a flat plate with a three-dimensional isolated roughness element immersed in a laminar boundary layer flow. The roughness element with height of 0.1 times the boundary layer displacement thickness is located downstream from a disturbance source, which produces two-dimensional Tollmien-Schlichting waves. It is expected that different wave parameters, such as amplitude and frequency, as well as base flow conditions, could yield a wide range of scenarios. Although unable to induce transition to turbulence, this study shows the roughness influence on the evolution of the TS waves, such as scattering of the waves into oblique ones and weak distortion of the mean flow.*

Keywords: *roughness, boundary layer stability, laminar-turbulent transition, Direct Numerical Simulation*

1. INTRODUCTION

In this work, the nonlinear instability and transition to turbulent flow are investigated through a Direct Numerical Simulation (DNS) of two-dimensional Tollmien-Schlichting (TS) waves over a flat plate with a three-dimensional isolated roughness element immersed in a laminar boundary layer flow.

Similar structures are commonly found on aircraft surfaces and can influence their drag coefficient if transition is induced from the laminar regime to turbulent in the boundary layer. Prevention of numerous drag sources like these, although relatively small, is a challenge that could lead to saving on fuel and operating costs.

There is a large number of factors that influence on transition, several of which are interdependent. The study of each aspect individually promotes a better understanding of the complete mechanism and allows predictive modeling of phenomena, a great advantage in the aeronautical industry. In boundary layer flows, transition is often caused by primary instabilities and, as a consequence, the amplification of secondary instabilities. For small Mach numbers, the main primary instability source of these flows is the two-dimensional TS wave. Upon reaching certain amplitude values, these waves generate three-dimensional disturbances with amplification rates that are much higher than the primary modes, which can quickly lead to transition in some cases.

Thus, the objective of the current work is to develop of a suitable three-dimensional mesh with the DNS code. A roughness element will be located downstream from a disturbance source, which produces two-dimensional TS waves that could generate non-linear structures or even transition to turbulence.

2. REVIEW

Early works investigated roughness and imperfections on the surface of airfoils with zero pressure gradient or flat plates as elements that promoted transition from laminar to turbulent flow. Wind tunnel experiments from Fage (1943), Tani (1961), Tani (1969) and those shown in Dryden (1953) indicated that a smoother surface influenced in the conservation of stability in a laminar boundary layer. Therefore, it was of great importance to establish the highest height h of the structures that could be tolerated without influencing the transition, affecting downstream flow. It was also determined that for higher flow speeds, the distance between roughness and the transition point was gradually reduced.

On studies about two-dimensional roughnesses with disturbances, such as Klebanoff and Tidstrom (1972), Dovgal and Kozlov (1990) and Morkovin (1990), it was concluded that the flow region modified by the presence of the roughness is more sensitive to destabilizing influences. The degree of instability was dependent on the velocity profile and its interaction with the roughness geometry. The presence of waves with small oscillation amplitudes in the roughness region, around 1% of the velocity on the outer edge of the boundary layer U_0 , already proved strong influence on transition.

Comparing with studies on three-dimensional roughnesses, such as Morkovin (1990), Klebanoff *et al.* (1992), Délerly (2001), Plogmann *et al.* (2014) and de Paula *et al.* (2017), the results are even more complex and distinct from the two-dimensional cases for any Reynolds number. For Morkovin (1990), the affected region after the roughness is shorter, but even more sensitive to disturbances, promoting great amplification of the fundamental modes. A vortex structure is generated around the roughness, forming streamwise vortices that induce downwash along the centerline of the wake.

According to Plogmann *et al.* (2014), the growth of fundamental modes near the roughness is recovered at a sufficient distance from it, regaining linear stability characteristics. It was observed that the originally two-dimensional TS waves that interacted with the roughness and had fundamental oblique modes amplified turned into three-dimensional waves. The amplification of the wave was not constant in the transversal direction, having local and possibly periodic values in that direction. According to the classification on Plogmann *et al.* (2014), the roughness of medium height is between $h \sim 0$ and $h \sim \delta^*$, and presents non-linear receptivity. In this height range, the vortex structure that is formed around the roughness and the downwash region are well defined, but are generally not enough to cause the transition of the boundary layer, being damped along the flow.

The works of Ustinov (1995), Crouch (1997), Wörner *et al.* (2003), Wang (2004) and Rist and Jäger (2006) investigate the secondary instability generated by the interaction between a two-dimensional TS wave and three-dimensional roughness. There is scattering of the TS waves, producing unsteady three-dimensional disturbances that turn into growing secondary instability modes, predicted to be only on the roughness near field.

3. METHODOLOGY

The numerical simulations were performed by a DNS for the compressible Navier-Stokes equations, developed by the Group of Aeroacoustics, Transition and Turbulence (GATT) of the Department of Aeronautical Engineering of the São Carlos School of Engineering, University of São Paulo (EESC-USP). The main works that present the development and validation of the DNS can be found in Bergamo (2014), Gaviria Martínez (2016), Mathias (2017), Mathias and Medeiros (2019).

In this work, the fourth order Runge-Kutta method is used for time marching. For the spatial derivatives, a fourth order compact spectral-like compact finite differences shown by Lele (1992) is used. The preprocessing is done in MATLAB and the main processing is written in FORTRAN.

The governing equations were defined in a three-dimensional domain (x, y, z) , and time (t) , in terms of density (ρ) , the three velocity components (u, v, w) , and internal energy (e) . The values presented here are non-dimensional, by the characteristic velocity at the outer edge of the boundary layer (U_0) , the boundary layer displacement thickness at the roughness position (δ_r^*) and initial density (ρ_0) .

For the boundary conditions, the inflow boundary is defined as an uniform flow at constant temperature and the pressure derivative is zero. In the outflow, pressure is kept constant and the second derivative is null for the other variables. The outer flow condition on the wall-normal direction sets the second derivative of all variables to zero. The outerflow for the span-wise direction sets the derivative of all variables to zero, except for w at Z_{min} , set to zero, for symmetry.

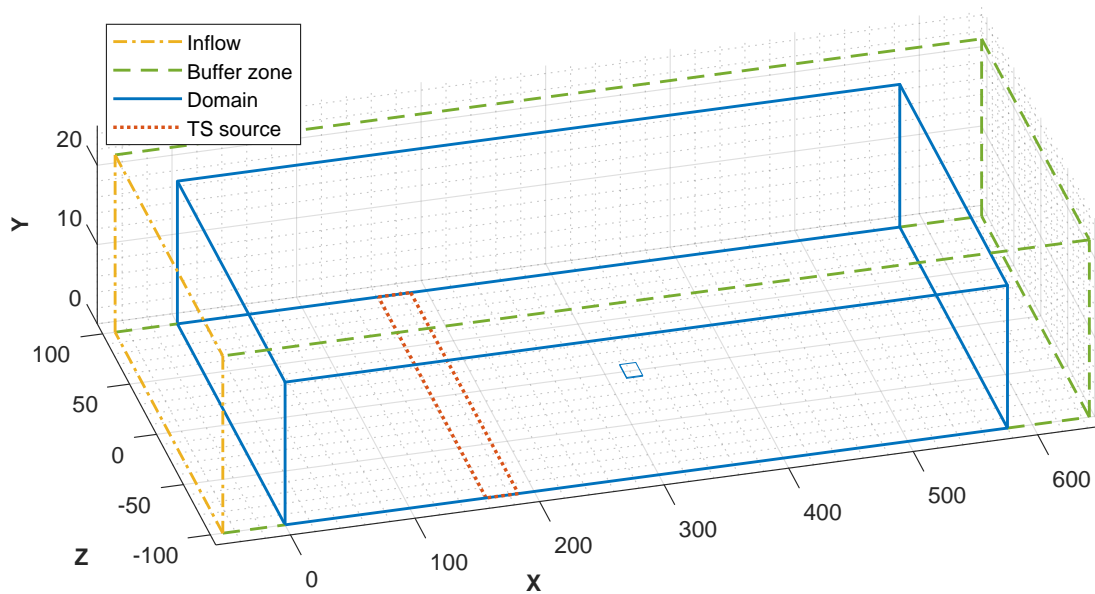


Figure 1. Non-dimensional illustration of the domain (Mesh 2)

For the walls, including the roughness, there are no-slip and no-penetration conditions for velocity, the pressure gradient is zero in the normal direction and the temperature is fixed. From $X = -50$ to $X = 0$ there is a free-slip region in the wall, necessary to accommodate the flow before the boundary layer starts forming.

The initial condition is a Blasius boundary layer at constant temperature and pressure. The characteristic Mach and Reynolds numbers are, respectively, $M = 0.3$ and $Re = 950$.

A square-base prism shaped roughness was centered on the Z coordinate of a flat plate, according to Fig. 1. Upstream from the roughness, there is a region, represented by the dotted line, capable of generating disturbances that travel downstream, interacting with the roughness.

Some flow parameters were taken from the experimental works by de Paula (2007) and de Paula *et al.* (2017), such as: Reynolds number in the position of the wave generator $Re_{\delta_{TS}^*} = 700$, Reynolds number at the roughness position $Re_{\delta_r^*} = 950$, velocity at the outer edge of the boundary layer $U_0 = 27.5 \text{ m/s}$, roughness diameter $d = 10 \text{ mm}$ and displacement thickness at the experimental roughness location $\delta_r^* = 0.55 \text{ mm}$.

The roughness width was defined as the width of a square circumscribed of a circle with the diameter of the experimental cylinder. Its height was defined as 10% of the boundary layer displacement thickness at the position of the center of the roughness on a flat plate, that is, $0.1\delta_r^*$.

The meshes are Cartesian and initially uniform, which can be stretched in certain regions, increasing the density of nodes as needed. As seen on Fig. 2, four different meshes were used to verify grid independence for the base flow.

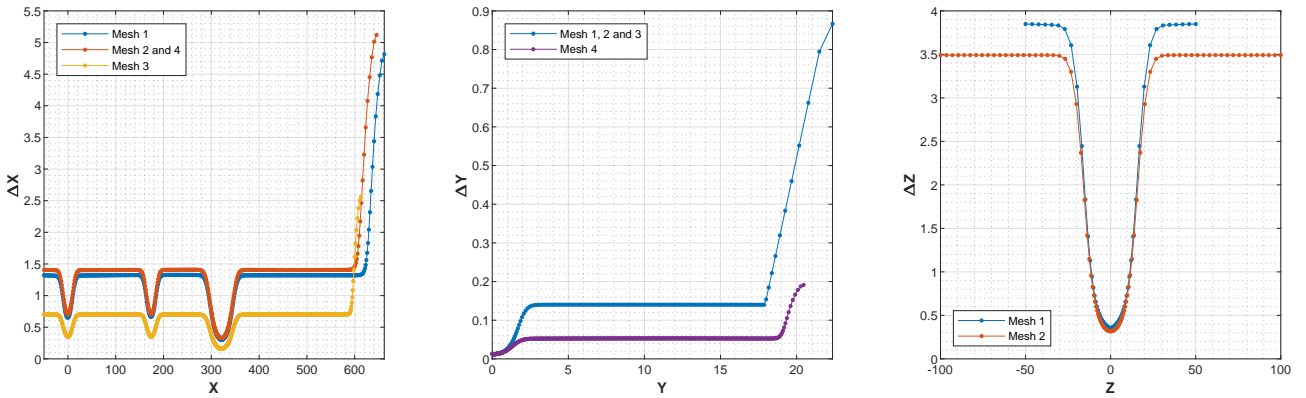


Figure 2. Grid spacing

| | Mesh 1 (3D) | Mesh 2 (3D) | Mesh 3 (2D) | Mesh 4 (2D) |
|--------------------------|-------------------|-------------------|--------------------|--------------------|
| ΔX_{min} | 0.3043 | 0.3292 | 0.1621 | 0.3292 |
| ΔX_{max} | 4.8147 | 5.1206 | 2.5579 | 5.1206 |
| ΔY_{min} | 0.0123 | 0.0123 | 0.0123 | 0.0121 |
| ΔY_{max} | 0.8667 | 0.8667 | 0.8667 | 0.1913 |
| ΔZ_{min} | 0.3500 | 0.3175 | - | - |
| ΔZ_{max} | 3.8488 | 3.4914 | - | - |
| X_{min} | -50 | -50 | -50 | -50 |
| X_{max} | 600 | 580 | 580 | 580 |
| Y_{min} | 0 | 0 | 0 | 0 |
| Y_{max} | 18 | 18 | 18 | 18 |
| Z_{min} | 0 | 0 | - | - |
| Z_{max} | 27 | 100 | - | - |
| Nodes in X | 600 | 550 | 1100 | 550 |
| Buffer zone nodes in X | 30 | 30 | 30 | 30 |
| Nodes in Y | 200 | 200 | 200 | 400 |
| Buffer zone nodes in Y | 10 | 10 | 10 | 30 |
| Nodes in Z | 37 | 55 | 1 | 1 |
| Total nodes | 4.9×10^6 | 6.7×10^6 | 2.37×10^5 | 2.49×10^5 |

Table 1. Meshes for the convergence analysis

In the X direction, the mesh is refined on three regions: around $X = 0$, in the wave generator region, between $X = 161.38$ and $X = 187.31$, and in the roughness region, between $X = 314.69$ and $X = 327.55$. The buffer zone

consists of the region from X_{max} to the end of the mesh, which is included to avoid problems in the simulation, such as reflections in the domain.

In Y , there is a region with an intense refinement along the height of the roughness, from $Y = 0$ to $Y = 0.1$. The buffer zone starts at $Y = 18$ and ends at the last node.

The simulated tree-dimensional meshes showed only the positive Z direction. As it is a symmetric problem, it is important to note that the results showing complete visualizations of the mesh are mirrored in $Z = 0$. Thus, the simulation time is greatly reduced and the results are not strongly affected. There is a refinement centered on $Z = 0$, ending in $Z = L/2$, which is half the width of the roughness.

On Fig. 3, the normalized streamwise velocity at $Y = 0.75\delta_r^*$, $Z = 0$ for all meshes, and at an arbitrary time after the periodic state has been established. It can be concluded that the solution converges and there is grid independence. As for the present work, mesh number 2 is chosen for the following analysis, for being the three-dimensional mesh with a wider range on the Z direction, most relevant to the downstream effects of the TS wave.

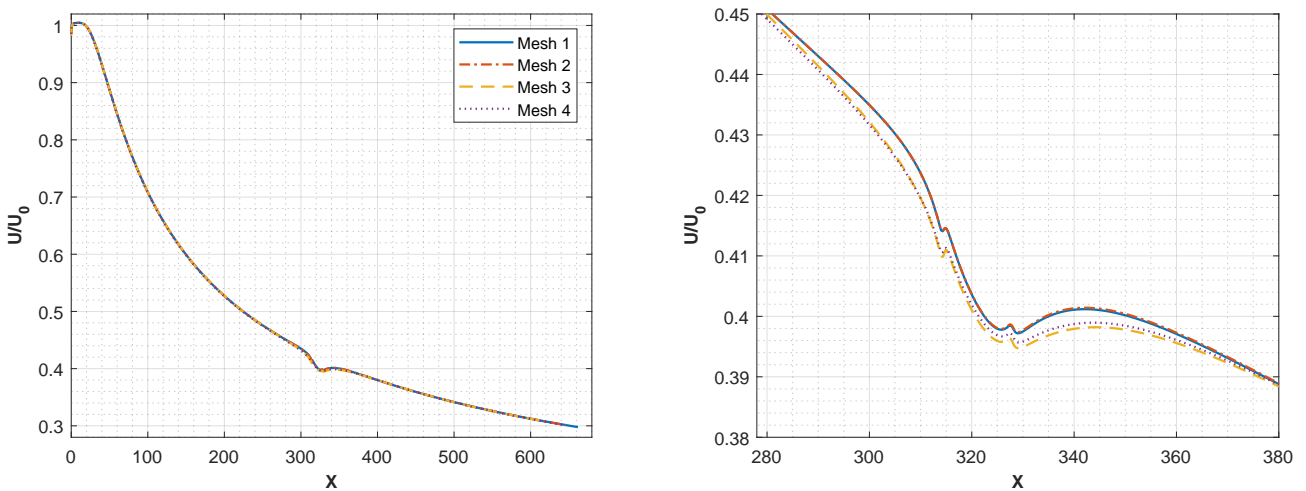


Figure 3. Wall-normal velocity component at $Y = 0.75\delta_r^*$ and $Z = 0$

4. RESULTS

4.1 Base Flow

The DNS was used to generate a three-dimensional base flow for a flat plate, for comparison, and a three-dimensional base flow with an isolated roughness element. The simulation of flat plate with roughness has a maximum relative error close to the order of 10^{-10} , an adequate value for a base flow simulation for the following analysis.

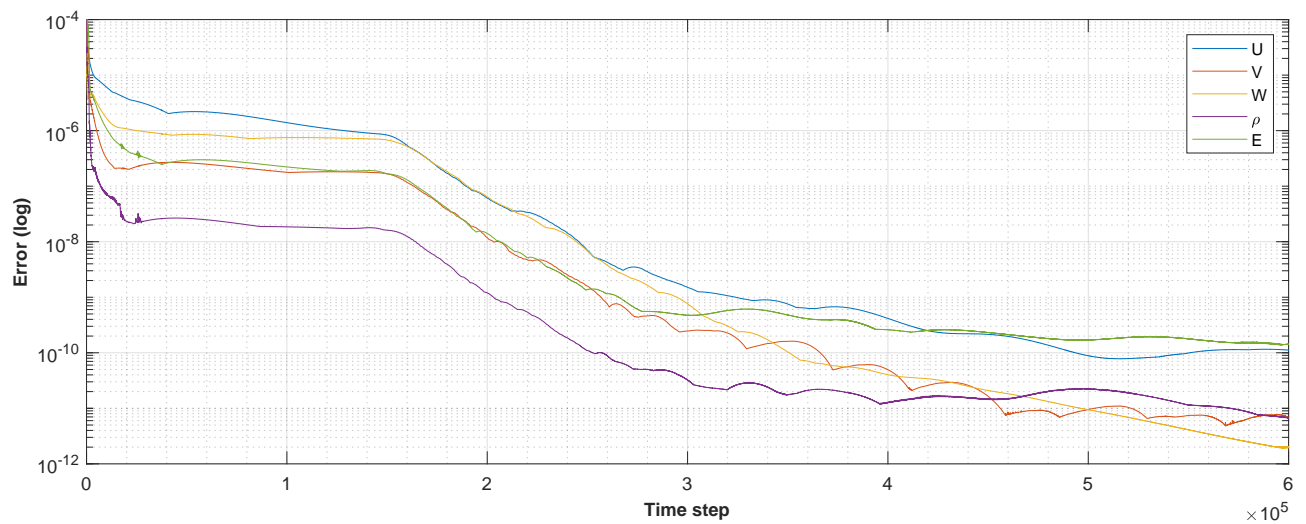


Figure 4. Relative error for three-dimensional base flow with isolated roughness

According to Fig. 5 and 6, the roughness effects on the boundary layer are concentrated in their proximity. There is a velocity deficit in just near the roughness, resuming the flat plate values to a small longitudinal distance, as expected. The displacement and momentum thickness of the boundary layer are be calculated using the equations in Schlichting and Gersten (2017).

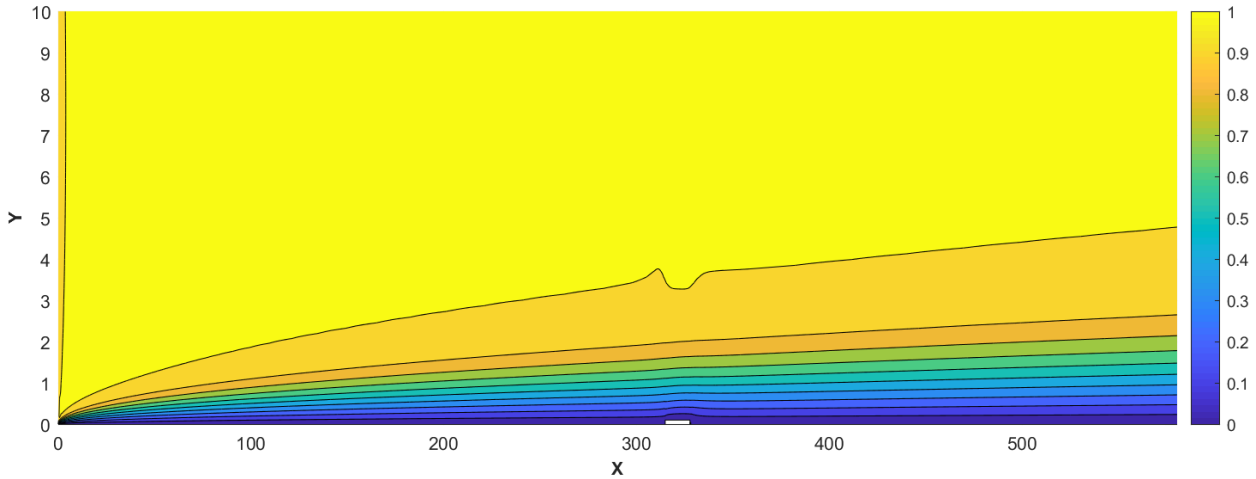


Figure 5. U/U_0 for the base flow on $Z = 0$

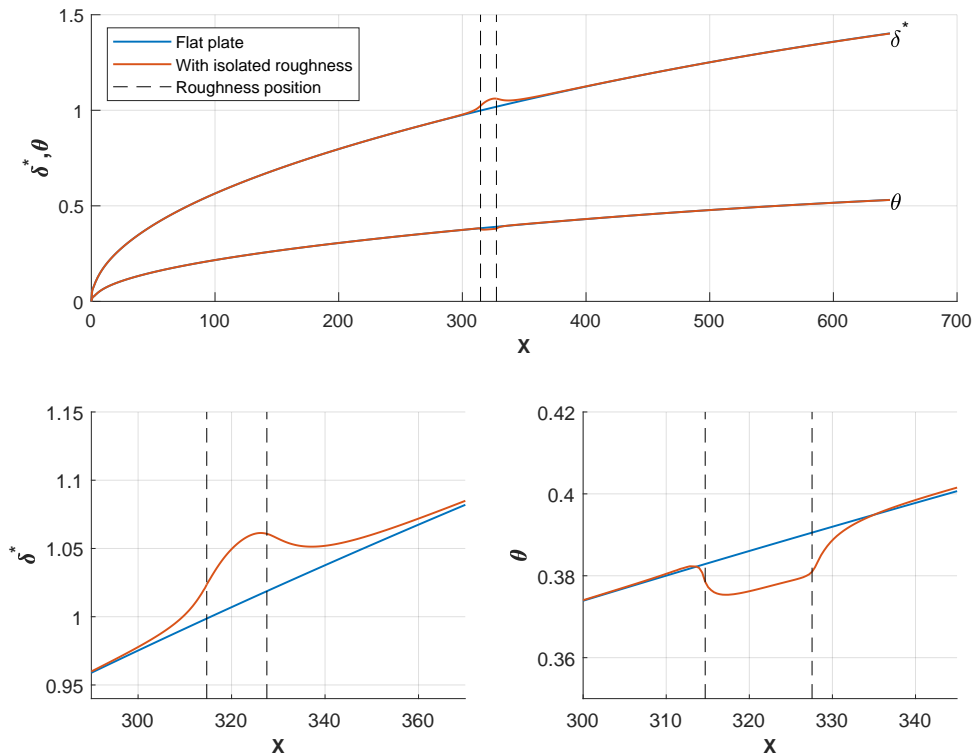


Figure 6. Displacement and momentum thickness on the boundary layer on $Z = 0$

4.2 Base Flow with TS Wave

On the base flow of a flat plate with three-dimensional roughness, a sinusoidal two-dimensional TS wave was generated with amplitude A_{0-2D} at the roughness position $A_{0-2D}/U_0 = 0.75\%$ and frequency $F = 9 \times 10^{-5}$. Positions downstream from the roughness are indicated by ΔX .

It is important to note that on Fig. 7, in particular, the amplitude value is obtained by subtracting the base flow of a three-dimensional flat plate, without roughness. In addition, the height of the represented roughness is not in scale with the graph, and the data presented are shown from $\Delta X = 25$ to 120 mm , according to the experimental results by de Paula *et al.* (2017).

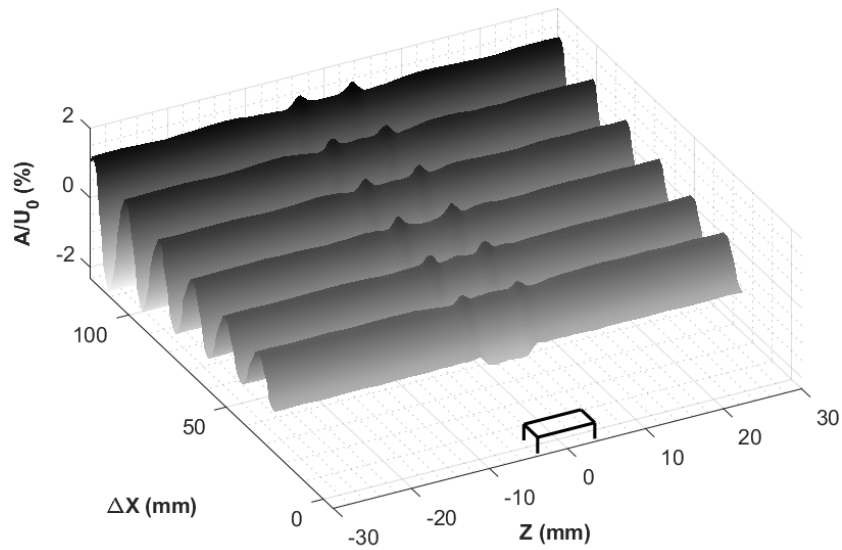


Figure 7. Streamwise evolution of TS wave amplitude at $y = 0.75\delta^*$

Results on Fig. 7 and show the roughness influence on the evolution of the TS waves, such as scattering of the waves into oblique ones, similar to the experiments. As the waves travel downstream from the roughness, the three-dimensional structures grow and expand on the span-wise direction.

On Fig. 8 it is clear the weak localized distortion of the mean flow. In this region, there could be a horseshoe vortex wrapped around the roughness, as mentioned by Morkovin (1990).

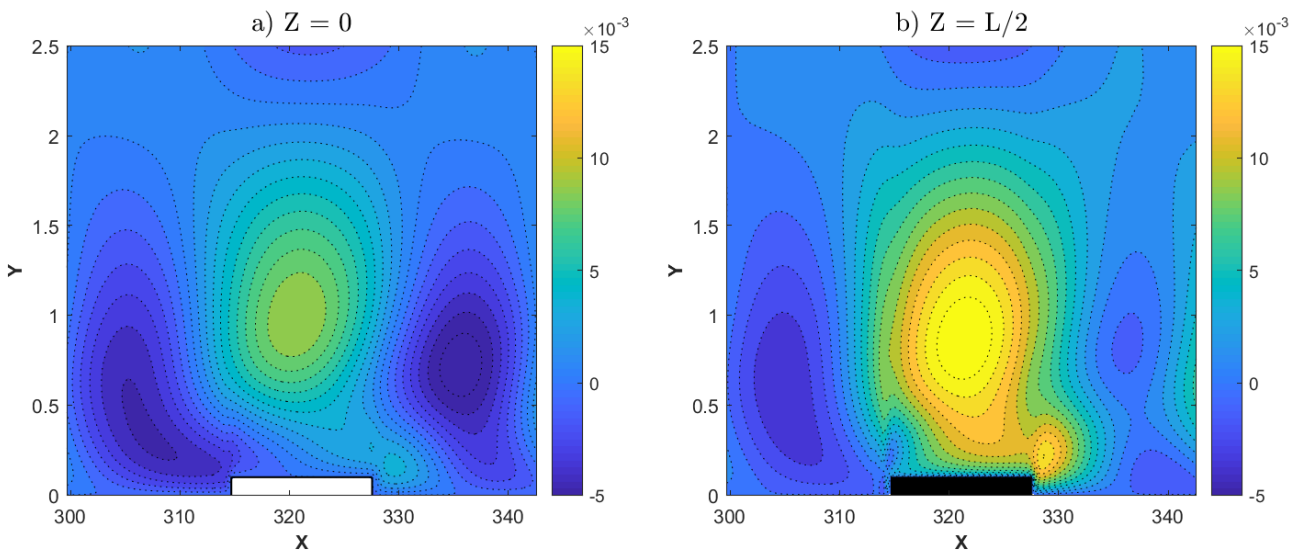


Figure 8. Fluctuations of velocity u'/U_0 on a flat plate with three-dimensional roughness and two-dimensional TS wave (sectional views)

5. CONCLUSIONS

It is safe to assume that the simulations reproduced well the characteristics of isolated roughness in the subsonic boundary layer with two-dimensional sinusoidal Tollmien-Schlichting wave. Results show as scattering of the waves into oblique ones, generating three-dimensional structures on an originally two-dimensional fluctuation, and weak distortion of the mean flow, localized on the roughness near field.

As no indication of transition from linear to turbulent boundary layer was identified, some parameters could be studied individually to try and achieve it, such as increasing the roughness height $h = 0.1\delta_r^*$, increasing the TS wave amplitude A_{0-2D}/U_0 and changing the Mach number $M = 0.3$. Also, with the results generated, it is possible to advance in the analysis of hydrodynamic instability in future works.

6. ACKNOWLEDGEMENTS

This study was financed in part by the Coordenação de Aperfeiçoamento de Pessoal de Nível Superior - Brasil (CAPES) - Finance Code 001.

F.H.T.H is sponsored by São Paulo Research Foundation (FAPESP/Brazil) grant #2018/02542-9.

M.S.M. is sponsored by São Paulo Research Foundation (FAPESP/Brazil) grant #2018/04584-0.

M.A.F.M. is sponsored by National Council for Scientific and Technological Development (CNPq/Brazil), grant #307956/2019-9.

We would like to thank the US Air Force Office of Scientific Research (AFOSR), grant FA9550-18-1-0112, managed by Dr. Geoff Andersen from SOARD (Southern Office of Aerospace Research and Development).

7. REFERENCES

- Bergamo, L.F., 2014. *Instabilidade hidrodinâmica linear do escoamento compressível em uma cavidade*. Master's thesis.
- Crouch, J.D., 1997. "Excitation of secondary instabilities in boundary layers". *Journal of Fluid Mechanics*, Vol. 336, pp. 245–266.
- de Paula, I.B., Würz, W., Mendonça, M.T. and Medeiros, M.A.F., 2017. "Interaction of instability waves and a three-dimensional roughness element in a boundary layer". *Journal of Fluid Mechanics*, Vol. 824, pp. 624–660.
- de Paula, I.B., 2007. *Influência de uma rugosidade tridimensional isolada na transição de uma camada limite sem gradiente de pressão*. Ph.D. thesis, Universidade de São Paulo.
- Délery, J.M., 2001. "Robert Legendre and Henri Werlé: Toward the Elucidation of Three-Dimensional Separation". *Annual Review of Fluid Mechanics*, Vol. 33, pp. 129–154.
- Dovgal, A.V. and Kozlov, V.V., 1990. "Hydrodynamic Instability and Receptivity of Small Scale Separation Regions". *Laminar-Turbulent Transition*, pp. 523–531.
- Dryden, H.L., 1953. "Review of Published Data on the Effect of Roughness on Transition from Laminar to Turbulent Flow". *Journal of the Aeronautical Sciences*, pp. 447–482.
- Fage, A., 1943. "The smallest size of spanwise surface corrugation which affects boundary-layer transition on an airfoil". *Aeronautical Research Council, R & M 2120*.
- Gaviria Martínez, G.A., 2016. *Towards natural transition in compressible boundary layers*. Ph.D. thesis, Universidade de São Paulo.
- Klebanoff, P.S., Cleveland, W.G. and Tidstrom, K.D., 1992. "On the evolution of a turbulent boundary layer induced by a three-dimensional roughness element". *Journal of Fluid Mechanics*, Vol. 237, No. 101, pp. 101–187.
- Klebanoff, P.S. and Tidstrom, K.D., 1972. "Mechanism by Which a Two-Dimensional Roughness Element Induces Boundary-Layer Transition". *The Physics of Fluids*, Vol. 15, No. 7, pp. 1173–1188.
- Lele, S.K., 1992. "Compact finite difference schemes with spectral-like resolution". *Journal of Computational Physics*, Vol. 103, pp. 16–42.
- Mathias, M.S., 2017. *Instability analysis of compressible flows over open cavities by a Jacobian-free numerical method*. Master's thesis, Universidade de São Paulo.
- Mathias, M.S. and Medeiros, M.F., 2019. *Global instability analysis of a boundary layer flow over a small cavity*.
- Morkovin, M.V., 1990. "On Roughness-Induced Transition: Facts, Views, and Speculations". pp. 281–295.
- Plogmann, B., Würz, W. and Krämer, E., 2014. "On the disturbance evolution downstream of a cylindrical roughness element". *Journal of Fluid Mechanics*, Vol. 758, pp. 238–286.
- Rist, U. and Jäger, A., 2006. "Unsteady disturbance generation and amplification in the boundary-layer flow behind a medium-sized roughness element". *IUTAM Symposium on Laminar-Turbulent Transition*, Vol. 78, pp. 293–298.
- Schlichting, H. and Gersten, K., 2017. *Boundary-Layer Theory*. Springer, Berlin, Heidelberg.
- Tani, I., 1961. "Effect of Two-Dimensional and Isolated Roughness on Laminar Flow". *Boundary Layer and Flow Control*, Vol. 2, pp. 637–656.
- Tani, I., 1969. "Boundary Layer Transition". *Annual Review of Fluid Mechanics*, Vol. 1, pp. 169–196.
- Ustinov, M.V., 1995. "Secondary Instability Modes Generated by a Tollmien-Schlichting Wave Scattering from a Bump". *Theoretical and Computational Fluid Dynamics*, Vol. 7, pp. 341–354.
- Wang, Y., 2004. *Instability and Transition of Boundary Layer Flows Disturbed by Steps and Bumps*. Ph.D. thesis, University of London.
- Wörner, A., Rist, U. and Wagner, S., 2003. "Humps/Steps Influence on Stability Characteristics of Two-Dimensional Laminar Boundary Layer". *AIAA Journal*, Vol. 41, No. 2, pp. 192–197.

8. RESPONSIBILITY NOTICE

The authors are the only responsible for the printed material included in this paper.